

Analysis of Stresses in Finite Anisotropic Panels with Centrally Located Cutouts

Vicki O. Britt
Structural Mechanics Division
NASA Langley Research Center
Hampton, Virginia

A 11511
220-39

ABSTRACT

P-21

A method for analyzing biaxial- and shear-loaded anisotropic rectangular panels with centrally located circular and elliptical cutouts is presented in the present paper. The method is based on Lekhnitskii's complex variable equations of plane elastostatics combined with a boundary collocation method and a Laurent series approximation. Results are presented for anisotropic panels with elliptical cutouts and subjected to combined shear and compression loading. The effects on the stress field of panel aspect ratio, anisotropy, cutout size, and cutout orientation are addressed. Angle-ply laminates, unidirectional off-axis laminates, and $[(\pm 45/0/90)_3]_s$, $[(\pm 45/0_2)_3]_s$, and $[(\pm 45/90_2)_3]_s$ laminates are examined.

INTRODUCTION

Stress distributions in laminated composite panels with cutouts are an important consideration in aircraft design and analysis. Cutouts are often necessary in aircraft structures to form access ports for electrical and mechanical systems. In addition, significant weight savings can be achieved through the introduction of cutouts in wing ribs and other aircraft components. The effects of cutout shape and orientation on the magnitude and distribution of the stress field are important in the design of these components. Presently, the majority of stress analysis methods are based on classical infinite plate theory or finite element analysis. Finite element analysis has been a popular approach to the stress analysis of finite-dimensional panels with cutouts (refs. 1, 2). These analyses produce accurate results, but they are costly methods of performing parametric studies in which several different materials and geometries must be considered. The method described in the present paper is an alternative to finite element analysis for panels with cutouts.

The method presented herein is based on the complex variable equations of plane elastostatics presented by Lekhnitskii (ref. 3). These equations are used in conjunction with a boundary collocation method and a Laurent series approximation to analyze the stress fields of anisotropic panels with centrally located cutouts. This method allows for biaxial, shear, and combined loading, and accommodates elliptical cutouts of arbitrary orientation, as well as circular cutouts.

An analytical study of the stress distribution in anisotropic panels with cutouts is presented to illustrate the versatility of the method, and some comparisons are made with

experimental data. The effects of panel aspect ratio, anisotropy, cutout size, and cutout orientation on the stress field are examined. Angle-ply laminates, unidirectional off-axis laminates, as well as $[(\pm 45/0/90)_3]_S$, $[(\pm 45/0_2)_3]_S$, and $[(\pm 45/90_2)_3]_S$ laminates, are considered.

SYMBOLS

A	ellipse minor axis
B_{kn}	constant coefficients of Laurent series
C_{mkn}	coefficients of Laurent series constant coefficients
D	circular cutout diameter and ellipse major axis
E_x	average elastic modulus in x-direction
E_y	average elastic modulus in y-direction
F	Airy stress function
F_m	applied forces at panel boundaries
G_{xy}	average shear modulus
L	panel length
S	arc length on interior or exterior boundary
W	panel width
X_n	x-component of boundary traction
Y_n	y-component of boundary traction
z_k	complex variable defined as $z_k = x + \mu_k y$
ε_x	average strain in x-direction
$\eta_{xy,x}$	coefficient of mutual influence of the second kind which characterizes shearing in the xy-plane caused by a normal stress in the x-direction
$\eta_{xy,y}$	coefficient of mutual influence of the second kind which characterizes shearing in the xy-plane caused by a normal stress in the y-direction
θ	fiber orientation angle
μ_k	complex roots of the characteristic equation
ν_{xy}	Poisson's ratio
Ψ	inclination angle of elliptical cutout
σ_x	average normal stress in the x-direction
σ_y	average normal stress in the y-direction
σ_{xy}	average shear stress
ϕ_k	functions of z_k which make up the stress function
Φ_k	first derivative of ϕ_k
ξ_i	transformation variable

A bar over a quantity denotes its complex conjugate.

ANALYSIS

Theory

The objective of this analysis is to develop a method for determining the stress distribution in a finite anisotropic panel with a centrally located elliptical cutout. The panel is loaded by in-plane forces which do not vary through the thickness, and a state of generalized plane stress is assumed. Thus, average material properties are employed in the present stress analysis, which is based on Lekhnitskii's complex variable equations (ref. 3). A complete description of this analysis is provided in references 4 and 5, and a summary follows.

The generalized biharmonic equation for an anisotropic material in terms of an Airy stress function, F , and the average material properties is

$$\frac{\partial^4 F}{\partial y^4} - 2\eta_{xy,x} \frac{\partial^4 F}{\partial y^3 \partial x} - \left(2\nu_{xy} - \frac{E_x}{G_{xy}}\right) \frac{\partial^4 F}{\partial y^2 \partial x^2} - 2\eta_{xy,y} \frac{E_x}{E_y} \frac{\partial^4 F}{\partial y \partial x^3} + \frac{E_x}{E_y} \frac{\partial^4 F}{\partial x^4} = 0$$

This biharmonic equation can be simplified using the transformation

$$z_1 = x + \mu_1 y \qquad z_2 = x + \mu_2 y$$

where μ_1, μ_2 , and their complex conjugates are the roots of the characteristic equation

$$\mu^4 - 2\eta_{xy,x} \mu^3 + \left(\frac{E_x}{G_{xy}} - 2\nu_{xy}\right) \mu^2 - 2\eta_{xy,y} \frac{E_x}{E_y} \mu + \frac{E_x}{E_y} = 0$$

Using the above transformation, the generalized biharmonic equation can be written as

$$\frac{\partial}{\partial z_1} \frac{\partial}{\partial z_2} \frac{\partial}{\partial z_1} \frac{\partial}{\partial z_2} F = 0$$

The solution for the stress function, F , is

$$F = \phi_1(z_1) + \phi_2(z_2) + \overline{\phi_1(z_1)} + \overline{\phi_2(z_2)}$$

Applied displacements or tractions along the panel boundary can be related to the complex-valued stress function. In this paper, only traction boundary conditions are considered. The boundary tractions in the x -direction, X_n , and in the y -direction, Y_n , are related to the stress function by

$$2\text{Re} [\Phi_1(z_1) + \Phi_2(z_2)] \Big|_{z_0}^z = \pm \left(- \int_0^S Y_n dS \right)$$

$$2\text{Re} [\mu_1 \Phi_1(z_1) + \mu_2 \Phi_2(z_2)] \Big|_{z_0}^z = \pm \int_0^S X_n dS$$

where S is the length of the boundary arc that begins at a point z_0 and ends at z , and $\Phi_k(z_k)$ is defined as

$$\Phi_k(z_k) = \frac{\partial \phi_k}{\partial z_k}$$

If the value of this stress function is known for every point within the panel boundaries, the stress distribution in the panel can be determined. In the present analysis, this stress function is represented by a truncated Laurent series containing unknown constant coefficients:

$$\Phi_k(z_k) = \sum_{-N}^N B_{kn} z_k^n$$

The resultant force on every arc of the interior and exterior boundaries is known and, therefore, Lekhnitskii's force equations can be used to solve for the unknown coefficients through boundary collocation. Satisfying the force loading conditions along the interior and exterior panel boundaries results in a system of equations that can be solved for the unknown Laurent series constants:

$$[C_{mkn}] \{ B_{kn} \} = \{ F_m \}$$

where B_{kn} are the unknown Laurent series constants, C_{mkn} are the coefficients of the Laurent series constants, and F_m are the applied force resultants. In order to improve solution convergence without increasing computation time, a least squares approach is implemented. The least squares method allows for an increase in the number of force equations

considered without an increase in the number of terms in the Laurent series. In the present case, twice as many equations as unknowns are considered; therefore,

[C_{mkn}] is a 16N x 8N matrix
 { B_{kn} } is an 8N vector
 { F_m } is a 16N vector

To solve the system of equations for the unknown Laurent series coefficients, each side of the matrix equation is multiplied by the transpose of [C_{mkn}]. To improve the conditioning of the system matrix, the following mapping function which maps all of the points inside the panel boundaries to the exterior of a unit circle is used:

$$\xi_i = \frac{1}{A - i\mu_i D} \left(z_i + \sqrt{z_i^2 - A^2 - \mu_i^2 D^2} \right) \quad i = 1, 2$$

where D is the major axis of the elliptical cutout, and A is the minor axis. The use of this mapping function eliminates the problem of small numbers being raised to high powers. After the system of linear algebraic equations is solved for the Laurent series constants, the average stresses in the panel can be calculated using the following stress equations:

$$\sigma_x = \frac{\partial^2 F}{\partial y^2} = 2\text{Re} [\mu_1^2 \Phi_1'(z_1) + \mu_2^2 \Phi_2'(z_2)]$$

$$\sigma_y = \frac{\partial^2 F}{\partial x^2} = 2\text{Re} [\Phi_1'(z_1) + \Phi_2'(z_2)]$$

$$\sigma_{xy} = -\frac{\partial^2 F}{\partial x \partial y} = -2\text{Re} [\mu_1 \Phi_1'(z_1) + \mu_2 \Phi_2'(z_2)]$$

Model

A FORTRAN program was written to implement the present analysis. The configuration analyzed consists of a rectangular panel with a centrally located cutout as shown in figure 1. The panel is of length L (in the x-direction) and of width W. The panel has either a circular or an elliptical cutout at its center. The circular cutout is of diameter D; the elliptical cutout has a major axis D and a minor axis A. The major axis of the ellipse may be

inclined at some angle Ψ to the y-axis or may be aligned with the y-axis. The panel is subjected to an applied shear stress, σ_{xy}^o , and/or an applied compressive stress, σ_x^o . In this study, when both shear and compression stresses are applied, they are equal in magnitude. The boundary of the cutout is assumed to be traction-free. The lamina fiber angles, θ , are measured with respect to the x-axis.

RESULTS AND DISCUSSION

Comparison with Experiment

To assess the accuracy of the current analytical approach, comparisons are made between experimental data and analytical results. The stress distribution near a circular cutout in a rectangular orthotropic panel with a uniaxial applied compressive stress is shown in figure 2. The $(\pm 45/0_2/\pm 45/0_2/\pm 45/0/90)_2S$ graphite-epoxy laminate has a width of 4.49 inches, a length of 10 inches, and cutout-diameter-to-panel-width ratios, D/W , of 0.11, 0.17, 0.22, and 0.33. Normal stress along the y-axis, $\sigma_x(0,y)$, normalized by the applied compressive stress, σ_x^o , is plotted as a function of the distance from the center of the panel, y , normalized by half the panel width, $W/2$. The analytical results are represented by solid lines, and the experimental data are represented by symbols. The experimental data were obtained from a study presented in reference 6. The analytical results agree well with the experimental data.

A comparison between analytical and experimental data is also made for a square $[(\pm 45/0/90)_3]_S$ graphite-thermoplastic laminate subjected to an applied shear stress, σ_{xy}^o . The panel has a width of 12 inches and cutout-diameter-to-panel-width ratios, D/W , of 0.063, 0.125, and 0.25. The normal strain along the y' -axis, $\epsilon_x(0,y')$, is plotted in figure 3 as a function of the nondimensional distance from the center of the panel, y'/W . For the purpose of this comparison, the panel is oriented at a 45° angle to the y-axis as shown in figure 3. The analytical results are represented by solid lines, and the experimental data from reference 7 are represented by symbols. The analytical results agree reasonably well with the experimental data; differences between analytical and experimental results are suspected to be largely due to the manner in which the load is introduced. In the analysis, a uniform shear stress is applied to the panel boundaries. In the experiment, loads are introduced through the use of a picture frame test fixture, which tends to concentrate the loads at the panel corners.

Analytical Study

To demonstrate the capabilities of the analytical method, stresses are calculated for a range of panel dimensions, ply layups, and loading conditions. Results are presented in terms of a maximum stress value which is normalized by the corresponding applied stress. This maximum stress value is obtained by conducting a survey of stress values at numerous evenly-spaced points on the panel. Points inside the cutout region are excluded. The

laminates analyzed are made of Hercules, Inc. AS4/3502 graphite-epoxy unidirectional tape and the lamina properties for the laminates studied are presented in Table 1.

The FORTRAN program which implements the present method consists of two lines of input describing the panel geometry, loading conditions, and average material properties. Due to the minimal amount of input, the following cases require very little user time for the creation of the models. In addition, the program run time is short enough that the program can be run interactively. Consequently, the present method exhibits a considerable advantage in time savings over finite element analyses in a study of this nature.

[(±45)₆]_S and (45)₂₄ laminates with circular cutouts.- As an example of the capabilities of the current analytical method, the extreme case of a unidirectional (45)₂₄ laminate exhibiting shear-extension coupling is analyzed and the results are compared with those for a more practical [(±45)₆]_S angle-ply laminate. The laminates contain circular cutouts and are subjected to a uniaxial compression load. The maximum normal stress, $(\sigma_x)_{\text{maximum}}$, normalized by the applied compressive stress, σ_x^o , is plotted in figure 4 as a function of panel aspect ratio, L/W , for different cutout diameters. The ratio L/W varies from one to three, and D/W is equal to 0.1, 0.3, and 0.6. The results for the [(±45)₆]_S laminate are represented by the solid line, the results for the (45)₂₄ laminate are represented by the dashed line, and the symbols, shown at points where analytical values are calculated, represent the different cutout diameters. As the cutout size increases, the panel aspect ratio has a significant effect on the maximum normal stresses, which are much higher for low aspect ratio panels than for high aspect ratio panels. The maximum normal stresses increase for large cutout sizes, and maximum normal stresses in the (45)₂₄ laminates are greater than maximum normal stresses in the [(±45)₆]_S laminates.

The analytical results for the [(±45)₆]_S and (45)₂₄ laminates subjected to an applied shear stress are shown in figure 5. The maximum shear stress, $(\sigma_{xy})_{\text{maximum}}$, normalized by the applied shear stress, σ_{xy}^o , is plotted as a function of panel aspect ratio, L/W , for D/W equal to 0.1, 0.3, and 0.6. Panel aspect ratio does not significantly influence the magnitude of the maximum shear stresses in a panel with a small cutout but becomes increasingly important as the cutout diameter grows larger. As with the compression-loaded laminates, the (45)₂₄ laminate has higher maximum shear stresses than the [(±45)₆]_S laminate under shear loading for the range of panel aspect ratios investigated in the present study.

Analytical results are also calculated for the [(±45)₆]_S and (45)₂₄ laminates subjected to combined compression and shear. The maximum normal stress, $(\sigma_x)_{\text{maximum}}$, normalized by the applied compressive stress, σ_x^o , is plotted in figure 6; and the maximum shear stress, $(\sigma_{xy})_{\text{maximum}}$, normalized by the applied shear stress, σ_{xy}^o , is plotted in figure 7. The maximum shear and normal stresses are plotted as functions of panel aspect ratio. An examination of the results for the laminates loaded in shear only and the laminates subjected to combined shear and compression loading reveals that the addition of the compression load to the shear-loaded panels does not greatly impact the trends and magnitudes of the maximum shear stresses. However, for combined loading conditions, the maximum normal stresses exhibit behavior radically different from the maximum normal stresses in the laminates loaded in compression only (see fig. 4). Under combined shear and compression loading, the maximum normal stresses in the (45)₂₄ laminates with D/W equal to 0.1 are lower than the maximum normal stresses in the [(±45)₆]_S laminates with the same D/W . For large cutouts and low panel aspect ratios, the maximum normal stresses in the (45)₂₄ laminates are larger

than the maximum normal stresses in the $[(\pm 45)_6]_S$ laminates. However, for large cutouts and high aspect ratios, the maximum normal stresses in the $[(\pm 45)_6]_S$ laminates are higher than the maximum normal stresses in the $(45)_{24}$ laminates.

$[(\pm 45/0/90)_3]_S$, $[(\pm 45/0_2)_3]_S$ and $[(\pm 45/90_2)_3]_S$ laminates with circular cutouts. - In order to study the effects of panel aspect ratio and cutout size on the stress field of some commonly used laminates, $[(\pm 45/0/90)_3]_S$, $[(\pm 45/0_2)_3]_S$, and $[(\pm 45/90_2)_3]_S$ laminates subjected to compression, shear, and combined loads are analyzed. The maximum normal stress, $(\sigma_x)_{\text{maximum}}$, normalized by the applied compressive stress, σ_x^0 , is plotted in figure 8 as a function of panel aspect ratio for these three laminates subjected to a compression load for D/W equal to 0.1, 0.3, and 0.6. The 0° plies have the highest extensional modulus and, therefore, the $[(\pm 45/0_2)_3]_S$ laminate, which contains the most 0° plies of the laminates studied, has the highest maximum normal stresses for all cutout diameters. The $[(\pm 45/90_2)_3]_S$ laminate, which does not contain any 0° plies, has the lowest maximum normal stresses for all values of D/W . The panel aspect ratio, L/W , has a minimal effect on the results for laminates with D/W equal to 0.1. However, as the cutout diameter increases, the laminates with larger cutout diameters have very high maximum normal stresses at low panel aspect ratios, and these maximum normal stress values tend to coalesce as the panel aspect ratio increases.

The maximum shear stress, $(\sigma_{xy})_{\text{maximum}}$, normalized by the applied shear stress, σ_{xy}^0 , is plotted in figure 9 as a function of panel aspect ratio for the $[(\pm 45/0/90)_3]_S$, $[(\pm 45/0_2)_3]_S$, and $[(\pm 45/90_2)_3]_S$ laminates subjected to a shear load. For cutout-diameter-to-panel-width ratios, D/W , of 0.1 and 0.3, the $[(\pm 45/90_2)_3]_S$ laminate has the highest maximum shear stresses and the $[(\pm 45/0/90)_3]_S$ laminate has the lowest maximum shear stresses for the range of L/W considered. As the panel aspect ratio increases, this trend remains unchanged for D/W equal to 0.1 and 0.3. However, for D/W equal to 0.6, the ordering of the $[(\pm 45/0/90)_3]_S$, $[(\pm 45/0_2)_3]_S$, and $[(\pm 45/90_2)_3]_S$ laminates in terms of the highest and lowest maximum shear stresses changes as the panel aspect ratio increases. For low values of L/W , the same trend that is observed for laminates with D/W equal to 0.1 and 0.3 occurs for D/W equal to 0.6. As the panel aspect ratio begins to increase, the $[(\pm 45/90_2)_3]_S$ laminate continues to have the highest maximum shear stresses, but the $[(\pm 45/0_2)_3]_S$ laminate has the lowest maximum shear stresses. For a panel aspect ratio of three, the $[(\pm 45/0_2)_3]_S$ laminate has the highest maximum shear stress, and the $[(\pm 45/0/90)_3]_S$ laminate has the lowest maximum shear stress.

Results are also obtained for the $[(\pm 45/0/90)_3]_S$, $[(\pm 45/0_2)_3]_S$, and $[(\pm 45/90_2)_3]_S$ laminates subjected to combined shear and compression loads. The maximum normal stress, $(\sigma_x)_{\text{maximum}}$, normalized by the applied compressive stress, σ_x^0 , is plotted as a function of panel aspect ratio in figure 10. The addition of the shear load to the compression load increases the maximum normal stresses. For all values of D/W , the $[(\pm 45/0_2)_3]_S$ laminate still has the highest maximum normal stresses, and the $[(\pm 45/90_2)_3]_S$ laminate still has the lowest maximum normal stresses. However, the change in the magnitude of the maximum normal stresses as the panel aspect ratio increases is not as large for the combined load case as for the compression load case. Maximum shear stresses, $(\sigma_{xy})_{\text{maximum}}$, normalized by the applied shear stress, σ_{xy}^0 , are plotted as a function of panel aspect ratio in figure 11. The addition of the compression load to the shear load increases the maximum shear stresses in the laminates, but the general trends remain the same with one exception. For panel aspect ratios near 1.0, the $[(\pm 45/0_2)_3]_S$ laminate has higher maximum shear stresses than the $[(\pm 45/90_2)_3]_S$ laminate for D/W equal to 0.3 and 0.6. As expected from symmetry

considerations, the $[(\pm 45/90)_2]_3$ s and $[(\pm 45/0)_2]_3$ s laminates have identical maximum shear stress values for a panel aspect ratio of 1.0 when they are subjected to shear loading only (see fig. 9).

Angle-ply laminates with circular cutouts.- Angle-ply laminates with circular cutouts are analyzed in order to examine the effects of fiber angle orientation on the maximum stresses in panels subjected to shear, compression, and combined loads. In figure 12, maximum normal stresses, $(\sigma_x)_{\text{maximum}}$, normalized by the applied compressive stress, σ_x^0 , are plotted as a function of fiber angle, θ , for square, compression-loaded, angle-ply laminates with circular cutouts. The solid lines represent analytical results for D/W equal to 0.1, 0.3, and 0.6. The fiber angle, θ , for the $[(\pm\theta)_6]_s$ angle-ply laminate ranges from 0° to 90° . The maximum normal stresses are largest for a fiber angle of 0° , which coincides with the direction of the applied stress. The maximum normal stresses decrease steadily as the fiber angle is increased. This reduction in maximum normal stress values is attributed to the decrease in the extensional modulus of the angle-ply laminate as the fiber angle increases.

The maximum shear stresses, $(\sigma_{xy})_{\text{maximum}}$, normalized by the applied shear stress, σ_{xy}^0 , are plotted in figure 13 as a function of fiber angle, θ , for square, shear-loaded, angle-ply laminates with circular cutouts. The ratio D/W is equal to 0.1, 0.3, and 0.6, and θ ranges from 0° to 90° . In some cases, the exact maximum stress is probably not found because the laminate stresses are calculated at a finite number of points on the panel. This discretization problem can cause some waviness in the maximum stress curves. The largest maximum shear stresses occur for a fiber angle of about 45° and decrease to minimums at fiber angles of 0° and 90° . This behavior appears to be consistent with the decrease in the laminate shear modulus as the fiber angle changes from 45° .

Square angle-ply laminates with circular cutouts with D/W equal to 0.1, 0.3, and 0.6 are also analyzed for combined shear and compression loads. The maximum normal stress, $(\sigma_x)_{\text{maximum}}$, normalized by the applied compressive stress, σ_x^0 , and the maximum shear stress, $(\sigma_{xy})_{\text{maximum}}$, normalized by the applied shear stress, σ_{xy}^0 , are plotted as functions of fiber angle in figures 14 and 15, respectively. The maximum normal and shear stresses show significant increases in magnitude over the maximum normal and shear stresses for the single load cases. The highest maximum normal stresses occur at a fiber angle of 0° as they did in the laminates subjected to a compression load only. The highest maximum shear stress for laminates with cutout-diameter-to-panel-width ratios, D/W , equal to 0.1 occurs at a 45° fiber angle and shifts toward a fiber angle of 40° as D/W increases to 0.6.

Angle-ply laminates with elliptical cutouts.- Angle-ply laminates with elliptical cutouts are examined to assess the effects of cutout shape, size, and orientation on the maximum stresses. For this analysis, the ratio of the major axis of the ellipse, D , to the panel width, W , is given values of 0.1, 0.3, and 0.6. The ratio of the minor axis, A , to the major axis of the ellipse, D , is equal to 0.5, 0.75, and 1.0. The major axis of the elliptical cutout is inclined at an angle Ψ to the y -axis, and Ψ ranges from 0° to 90° . The maximum normal stress, $(\sigma_x)_{\text{maximum}}$, normalized by the applied compressive stress, σ_x^0 , is plotted as a function of Ψ for square, compression-loaded $[(\pm 30)_6]_s$, $[(\pm 45)_6]_s$, and $[(\pm 60)_6]_s$ laminates in figures 16, 17, and 18, respectively. Similar to the results for the angle-ply laminates with circular cutouts, the maximum normal stresses are highest in the $[(\pm 30)_6]_s$ laminate and decrease as the fiber angle increases. Laminates having elliptical cutouts inclined at small angles to the y -axis

have the largest maximum normal stresses, and, in most cases, these maximum normal stresses increase as A/D decreases. As Ψ is increased, the maximum normal stresses decrease in all of the laminates with elliptical cutouts. At large values of Ψ the maximum normal stresses decrease as A/D decreases.

Maximum shear stresses, $(\sigma_{xy})_{\text{maximum}}$, for the $[(\pm 30)_6]_S$, $[(\pm 45)_6]_S$, and $[(\pm 60)_6]_S$ laminates subjected to shear loads are normalized by the applied shear stress, σ_x^0 , and plotted as a function of the elliptical cutout orientation angle, Ψ , in figures 19, 20, and 21, respectively. The normalized maximum shear stress curves behave in a somewhat erratic manner. As mentioned previously, the laminate stresses are surveyed at a finite number of points. Therefore, the exact maximum stress is probably not always found, and some waviness in the maximum stress curves results. This waviness is magnified by the sensitivity of the value and location of the maximum shear stress to changes in Ψ , especially at low values of A/D . An example of this phenomenon is shown for the $[(\pm 45)_6]_S$ laminate in figures 22 through 25. The shear stress distribution and the maximum shear stress location for laminates with the major axis of the elliptical cutout inclined at 0° , 25° , and 45° are shown in figures 22, 23, and 24, respectively. In contrast, for circular cutouts the maximum shear stress location remains fixed. For example, the shear stress distribution for the $[(\pm 45)_6]_S$ laminate with a circular cutout is shown in figure 25.

Although the maximum shear stress curves do not vary smoothly, the general trends are discernable. In the case of the $[(\pm 30)_6]_S$ laminate, the maximum shear stresses occur when Ψ is about 30° for the smaller cutouts and about 45° for the largest cutout size. In the $[(\pm 45)_6]_S$ laminate, the maximum shear stresses occur when Ψ is equal to 45° for all cutout sizes. Under shear loading conditions, the maximum shear stresses in the $[(\pm 60)_6]_S$ laminate occur when Ψ is about 60° for small cutouts and about 45° for the largest cutout size. Of the three angle-ply laminates examined, the $[(\pm 45)_6]_S$ laminate has the overall highest maximum shear stresses. In all of the angle-ply laminates with cutout-major-axis-to-panel-width ratios, D/W , equal to 0.1 and 0.3, the maximum shear stresses increase as A/D decreases. For the laminates with D/W equal to 0.6, the maximum shear stress decreases as A/D decreases for values of Ψ near 0° and 90° . For some range of values of Ψ between 5° and 85° , depending on the particular laminate, the maximum shear stresses are highest for A/D equal to 0.5, and lowest for A/D equal to 0.75, with the maximum shear stresses for A/D equal to 1.0 falling between the two.

The maximum normal stresses, $(\sigma_x)_{\text{maximum}}$, normalized by the applied compressive stress, σ_x^0 , are plotted as a function of Ψ for the $[(\pm 30)_6]_S$, $[(\pm 45)_6]_S$, and $[(\pm 60)_6]_S$ laminates subjected to a combined shear and compression load in figures 26, 27, and 28, respectively. The addition of the shear load to the compression load causes the maximum normal stresses to increase to values approximately double the maximum normal stresses due to the compression load alone. In addition, the highest maximum normal stresses no longer occur near Ψ equal to 0° . Instead, they occur for values of Ψ ranging from 20° to 40° . Similar to the compression-loaded laminates, the $[(\pm 30)_6]_S$ laminate has the highest maximum normal stresses; and, in most cases, the maximum normal stresses in the laminates under combined loading increase as A/D decreases. The maximum shear stresses, $(\sigma_{xy})_{\text{maximum}}$, normalized by the applied shear stress, σ_{xy}^0 , for the laminates subjected to combined loads are shown as a function of Ψ in figures 29, 30, and 31. The addition of the compression load to the shear load increases the maximum shear stress values and changes the elliptical cutout rotation angle at which the highest maximum shear stresses occur. Similar to the shear-load-only

case, the $[(\pm 45)_6]_S$ laminate has the highest stresses, and a decrease in A/D results in an increase in the maximum shear stress.

CONCLUDING REMARKS

A method which combines Lekhnitskii's complex variable equations with boundary collocation and a Laurent series approximation is used to analyze the stress distributions in some finite anisotropic panels with centrally located cutouts. The maximum normal and shear stresses are found for panels with circular and elliptical cutouts and subjected to compression, shear, and combined loads. The effects of panel aspect ratio, anisotropy, cutout size, and cutout orientation on the magnitude and distribution of the stresses are examined. Angle-ply laminates, unidirectional off-axis laminates, as well as $[(\pm 45/0/90)_3]_S$, $[(\pm 45/0_2)_3]_S$, and $[(\pm 45/90_2)_3]_S$ laminates are studied in order to demonstrate the capabilities of the analytical method. To assess the accuracy of the method, analytical results are compared with experimental data for orthotropic panels with circular cutouts. The panels are subject to either compression or shear loading. In both cases, the analytical results show good agreement with the experimental data.

To demonstrate the flexibility of the analytical method with respect to material properties and panel geometry, several laminates subjected to compression, shear, and combined loads are analyzed. To study the effects of panel aspect ratio on laminate stresses, the limiting case of a $(45)_{24}$ laminate with a circular cutout is analyzed and compared to more common laminates constructed of 0° , 90° , and 45° plies. It is shown that the effect of panel aspect ratio on the magnitude of the stresses in panels with small cutouts is minimal, but as the cutout size increases, the effects become more significant. A study of square $[(\pm\theta)_6]_S$ angle-ply laminates with circular cutouts identifies relationships between shear and extensional moduli and the maximum normal and shear stresses. Angle-ply laminates with high extensional moduli, such as the $(0)_{24}$ laminate, have high maximum normal stresses when subjected to compression loading. As the fiber angle deviates from 0° , the maximum normal stresses decrease. Angle-ply laminates with high shear moduli, such as the $[(\pm 45)_6]_S$ laminate, have the highest maximum shear stresses when subjected to shear loading, and as the fiber angle deviates from 45° , the maximum shear stresses decrease.

A study of square angle-ply laminates with elliptical cutouts whose major axes are inclined to the panel coordinate system is conducted to demonstrate the ability of the current analytical method to accommodate different cutout geometries. The results indicate that the values of the maximum stresses depend on the relationships between several geometric factors and material properties. For example, the ellipse minor-axis-to-major-axis ratio has an effect on the maximum stresses that depends on the cutout size, the fiber angle of the angle-ply laminate, and the angle of inclination of the elliptical cutout. As the inclination of the elliptical cutout is varied, the stress distribution changes dramatically, especially for shear loading where the location of the maximum shear stress also changes.

The wide range of results obtained in the present study exemplifies the ability of the present method to adapt to many different panel sizes and cutout geometries. The method allows for biaxial, shear, and combined loads. While only traction loading conditions are considered in the present paper, the method is also capable of analyzing displacement

loading conditions. The flexibility of this method characterizes its main advantage over finite elements in the areas of structural design and optimization. In addition, the FORTRAN program that implements the present method requires minimal computer time and can run interactively. Because the present method requires only two lines of input to describe the model, user modeling time is significantly less than with finite element analyses.

REFERENCES

1. Hong, C. S.; and Crews, John H., Jr.: Stress-Concentration Factors for Finite Orthotropic Laminates With a Circular Hole and Uniaxial Loading. NASA TP 1469, May 1979.
2. Greszczuk, L. B.: Stress Concentrations and Failure Criteria for Orthotropic and Anisotropic Plates with Circular Openings. Composite Materials Testing and Design, ASTM STP 497, American Society for Testing and Materials, 1972.
3. Lekhnitskii, S. G.: Theory of Elasticity of an Anisotropic Body. Mir Publishers, Moscow, 1977.
4. Owen, Vicki L.; and Klang, Eric C.: Shear Buckling of Specially Orthotropic Plates With Centrally Located Cutouts. Presented at the Eighth DoD/NASA/FAA Conference on Fibrous Composites in Structural Design, NASA CP 3087, November 1989.
5. Owen, Vicki L.: Shear Buckling of Anisotropic Plates with Centrally Located Circular Cutouts. Masters Thesis, North Carolina State University, May 1990.
6. Rhodes, M. D.; Mikulas, M. M., Jr.; and McGowan, P. E.: Effects of Orthotropy and Width on the Compression Strength of Graphite-Epoxy Panels with Holes. AIAA Journal, Vol. 22, No. 9, September 1984, pp. 1283-1292.
7. Rouse, Marshall: Effect of Cutouts or Low-Speed Impact Damage on the Post-Buckling Behavior of Composite Plates Loaded in Shear. Presented at the AIAA/ASME/ASCE/AHA/ASC 31st Structures, Structural Dynamics, and Materials Conference, Long Beach, CA, April 2-4, 1990, AIAA Paper No. 90-0966-CP.

Table 1. Lamina properties of Hercules, Inc. AS4/3502 graphite-epoxy material

Longitudinal Young's Modulus, psi	18.5×10^6
Transverse Young's Modulus, psi	1.6×10^6
Shear Modulus, psi	0.832×10^6
Major Poisson's ratio	0.35

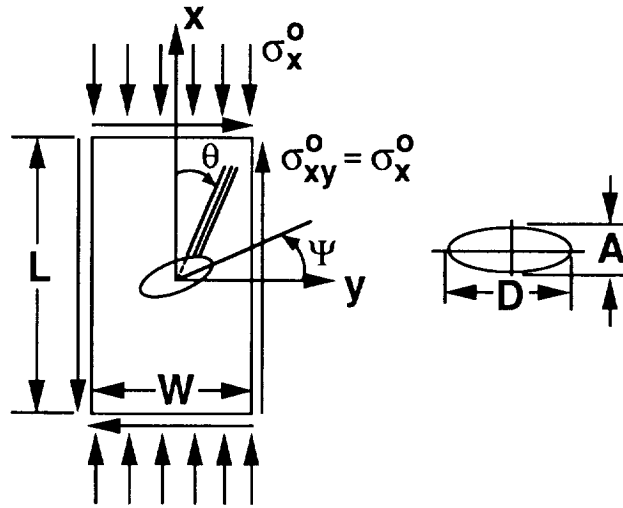


Fig. 1. Analytical model of a shear- and compression-loaded rectangular plate with a centrally located elliptical cutout inclined to the y-axis.

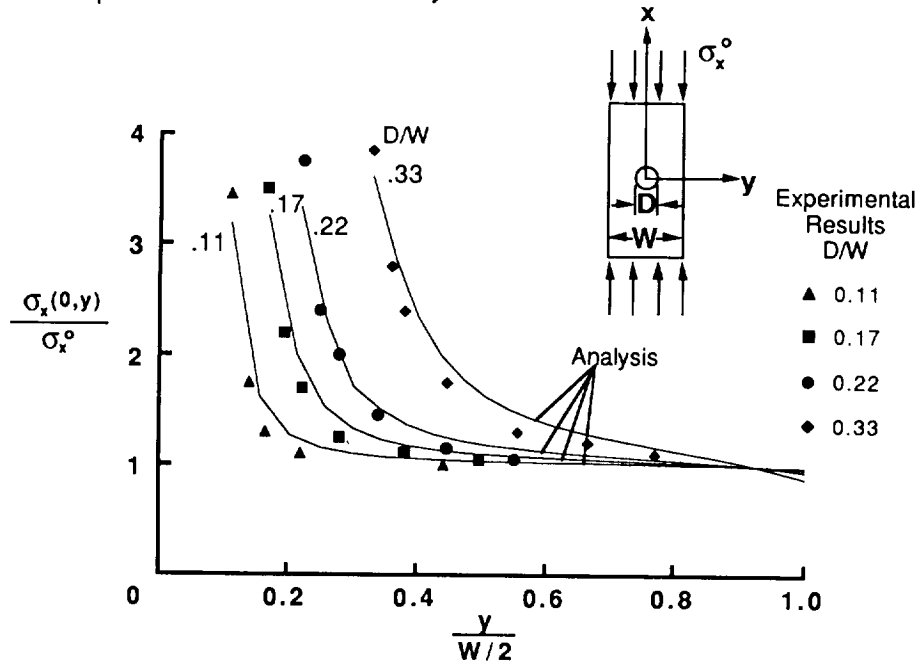


Fig. 2. Stress distribution near a circular cutout in a rectangular $(\pm 45/0_2/\pm 45/0_2/\pm 45/0/90)_{2S}$ panel under applied uniaxial compression (experimental data from reference 6).

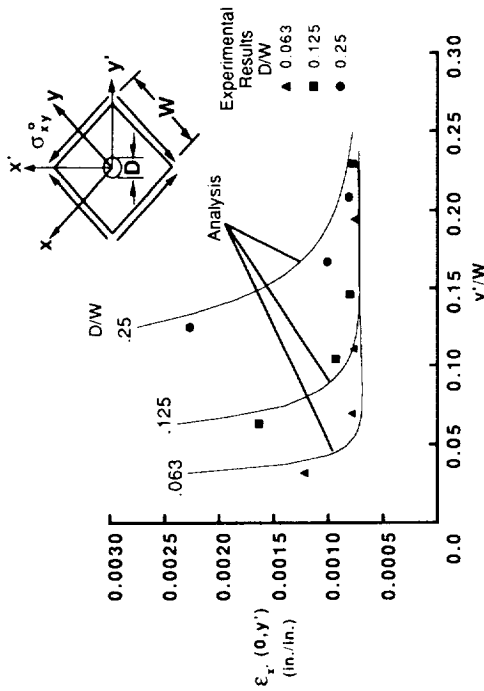


Fig. 3. Stress distribution near a circular cutout in a square [(±45/0/90)₂₄]_s panel under uniform shear loading (experimental data from reference 7).

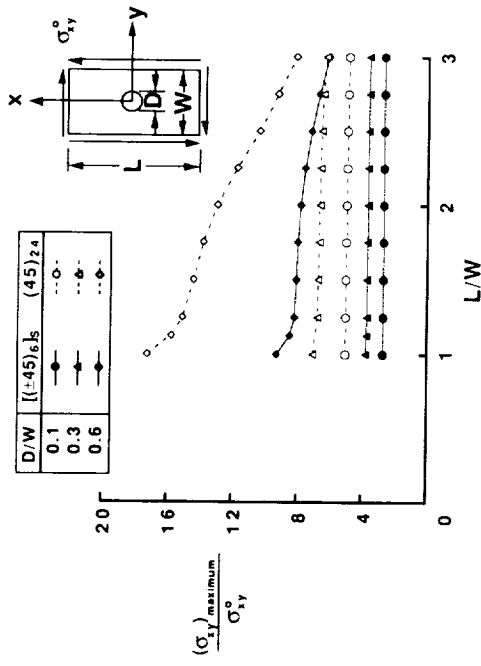


Fig. 5. Maximum shear stresses in rectangular shear-loaded [(±45)₆]_s and (45)₂₄ laminates with a circular cutout.

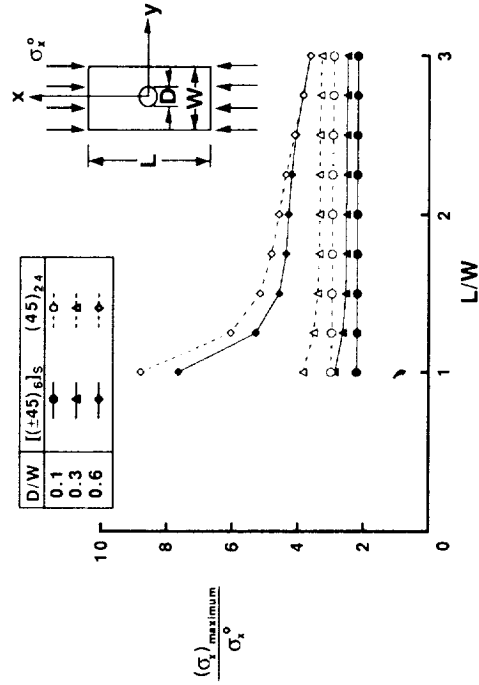


Fig. 4. Maximum normal stresses in rectangular uniaxial-compression-loaded [(±45)₆]_s and (45)₂₄ laminates with a circular cutout.

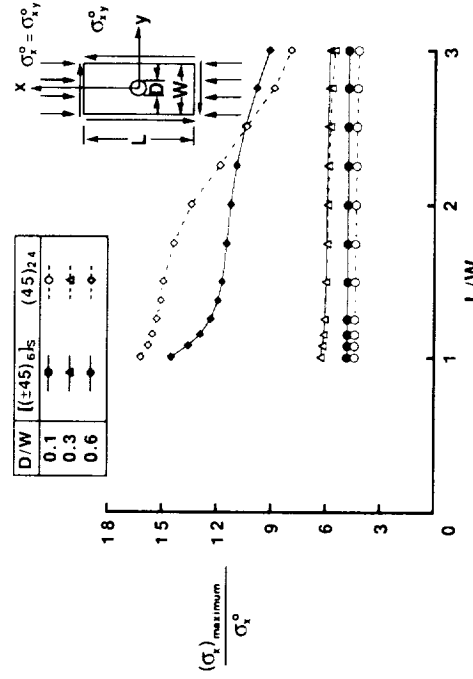


Fig. 6. Maximum normal stresses in rectangular compression- and shear-loaded [(±45)₆]_s and (45)₂₄ laminates with a circular cutout.

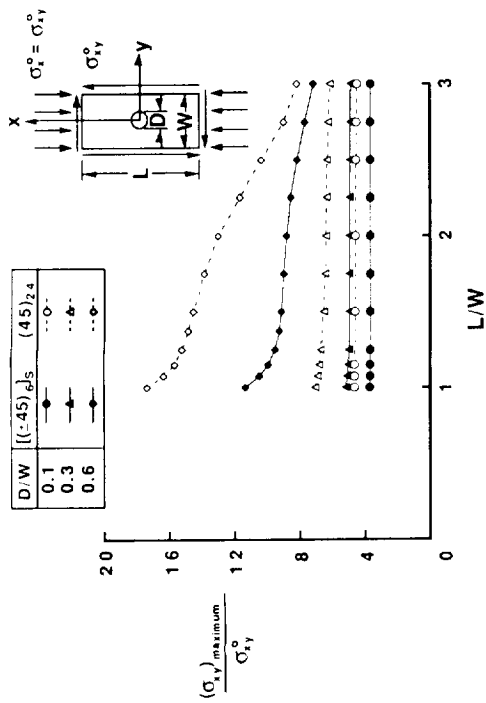


Fig. 7. Maximum shear stresses in rectangular compression- and shear-loaded $[(\pm 45)_2]_{24}$ and $(45)_{24}$ laminates with a circular cutout.

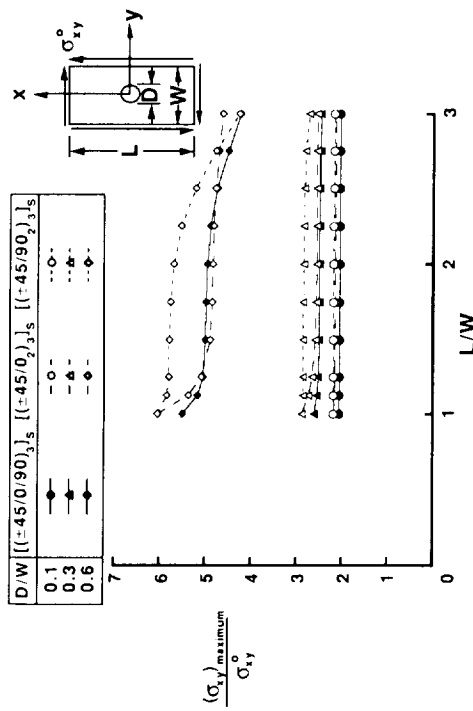


Fig. 9. Maximum shear stresses in rectangular shear-loaded $[(\pm 45/0/90)_3]_s$, $[(\pm 45/0)_3]_s$, and $[(\pm 45/0/2)_3]_s$ laminates with a circular cutout.

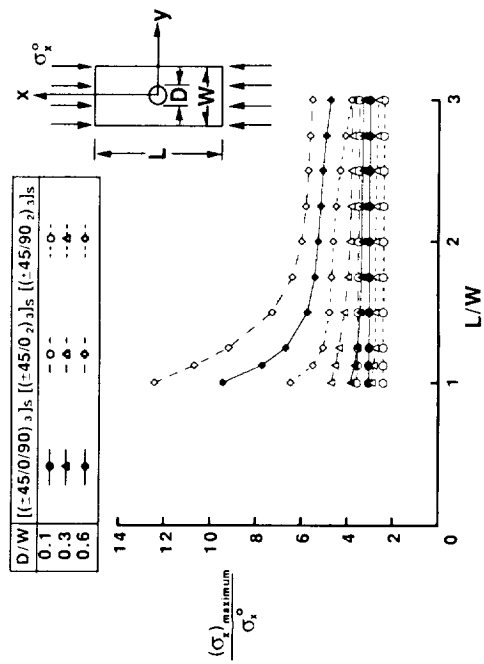


Fig. 8. Maximum normal stresses in rectangular compression-loaded $[(\pm 45/0/90)_3]_s$, $[(\pm 45/0)_3]_s$, and $[(\pm 45/0/2)_3]_s$ laminates with a circular cutout.

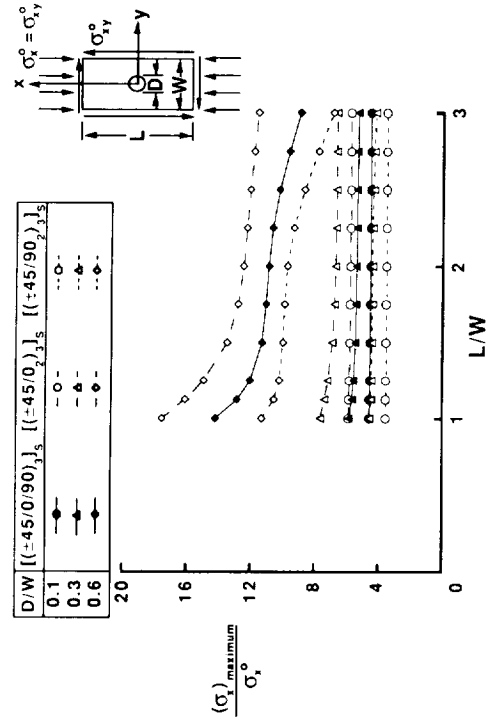


Fig. 10. Maximum normal stresses in rectangular compression- and shear-loaded $[(\pm 45/0/90)_3]_s$, $[(\pm 45/0)_3]_s$, and $[(\pm 45/0/2)_3]_s$ laminates with a circular cutout.

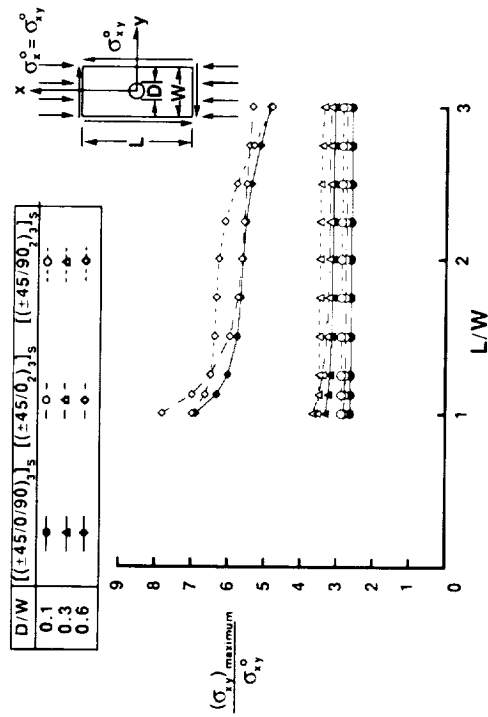


Fig. 11. Maximum shear stresses in rectangular compression- and shear-loaded [(±45/0/90)₂]_s, [(±45/0)₂]_s, and [(±45/90)₂]_s laminates with a circular cutout.

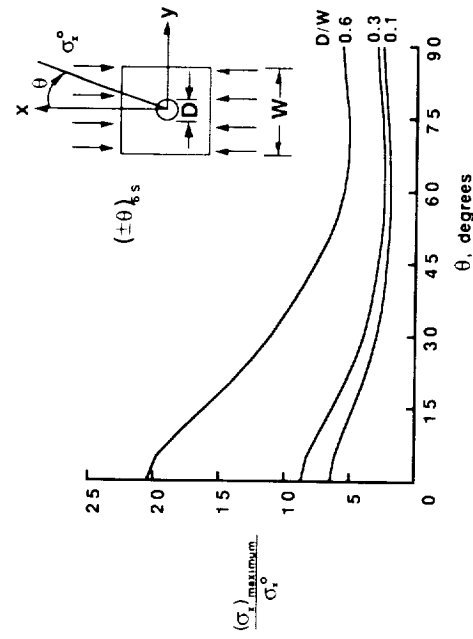


Fig. 12. Maximum normal stresses in square compression-loaded angle-ply laminates with a circular cutout.

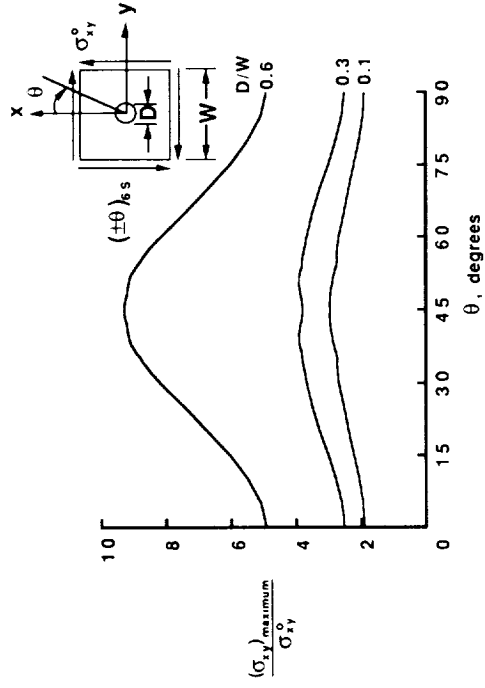


Fig. 13. Maximum shear stresses in square shear-loaded angle-ply laminates with a circular cutout.

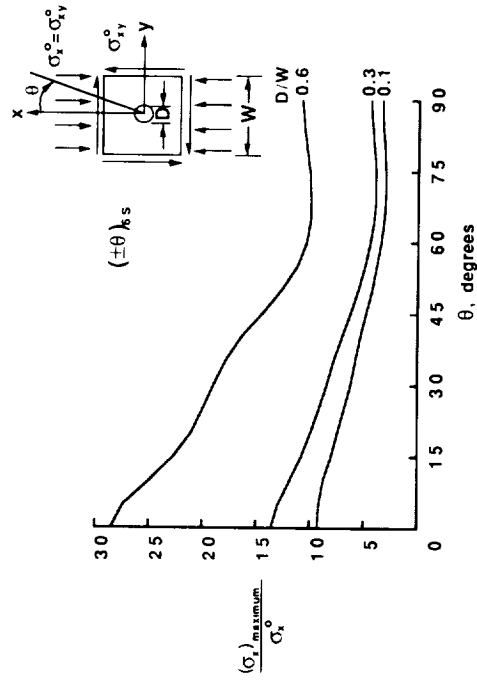


Fig. 14. Maximum normal stresses in square compression- and shear-loaded angle-ply laminates with a circular cutout.

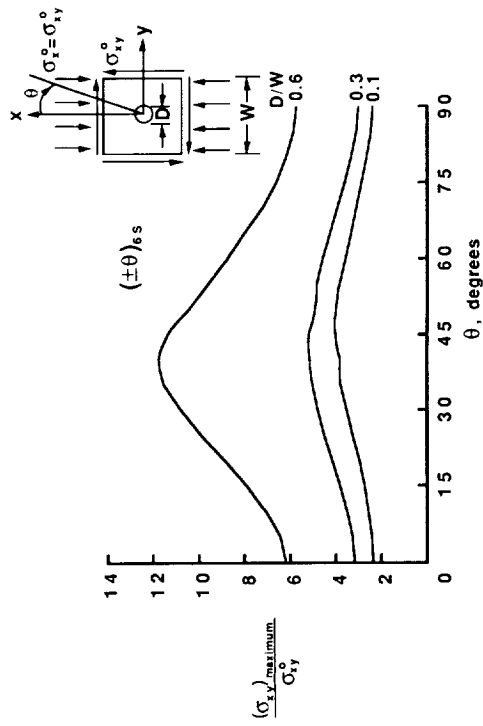


Fig. 15. Maximum shear stresses in square compression- and shear-loaded angle-ply laminates with a circular cutout.

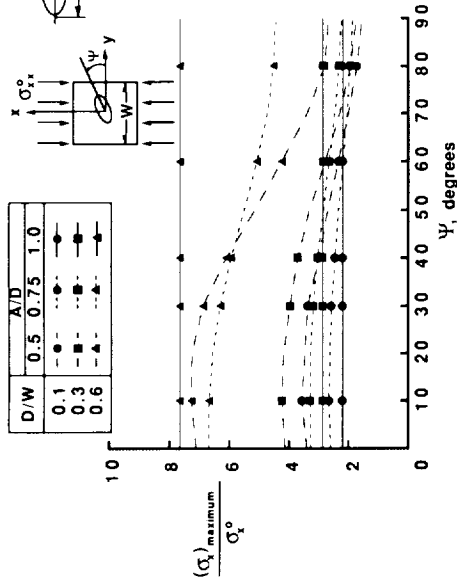


Fig. 17. Maximum normal stresses in a square compression-loaded $[(\pm 45)_6]_s$ laminate with an elliptical cutout inclined to the y-axis.

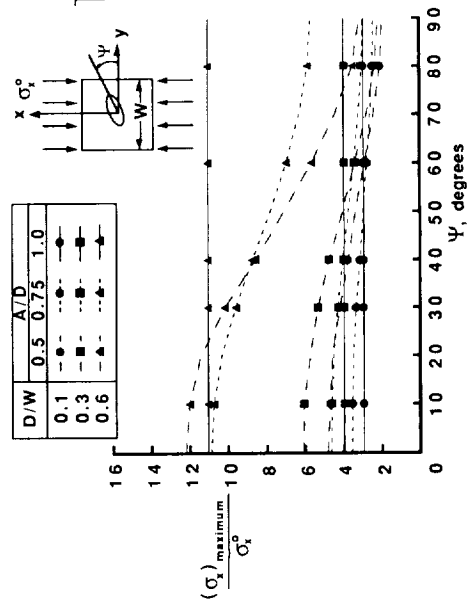


Fig. 16. Maximum normal stresses in a square compression-loaded $[(\pm 30)_6]_s$ laminate with an elliptical cutout inclined to the y-axis.

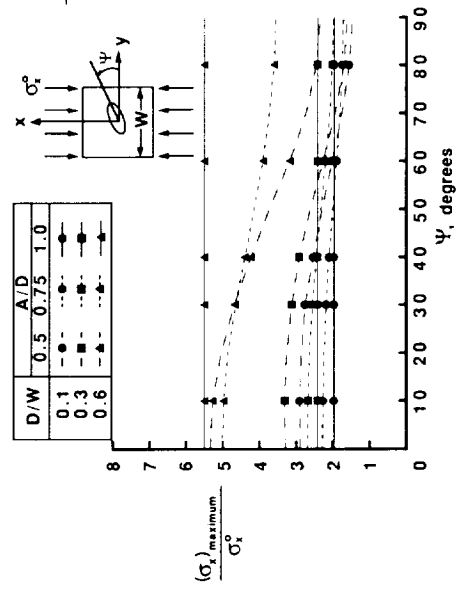


Fig. 18. Maximum normal stresses in a square compression-loaded $[(\pm 45)_6]_s$ laminate with an elliptical cutout inclined to the y-axis.

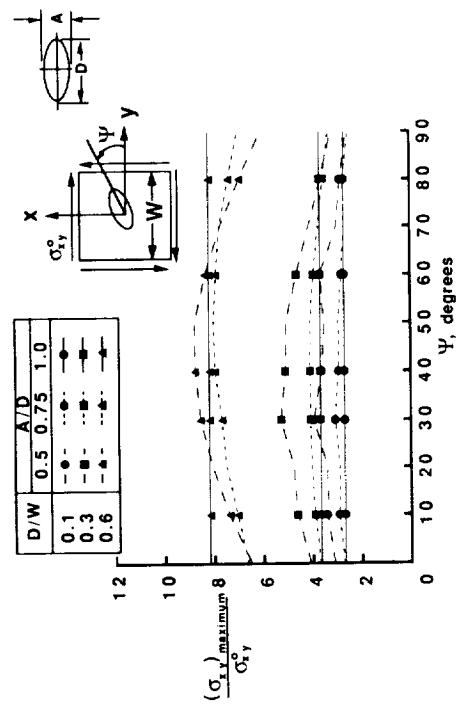


Fig. 19. Maximum shear stresses in a square shear-loaded [(±30)6]s laminate with an elliptical cutout inclined to the y-axis.

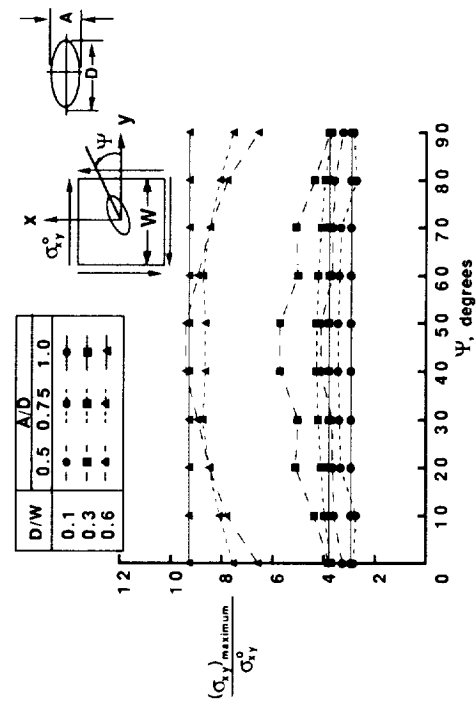


Fig. 20. Maximum shear stresses in a square shear-loaded [(±45)6]s laminate with an elliptical cutout inclined to the y-axis.

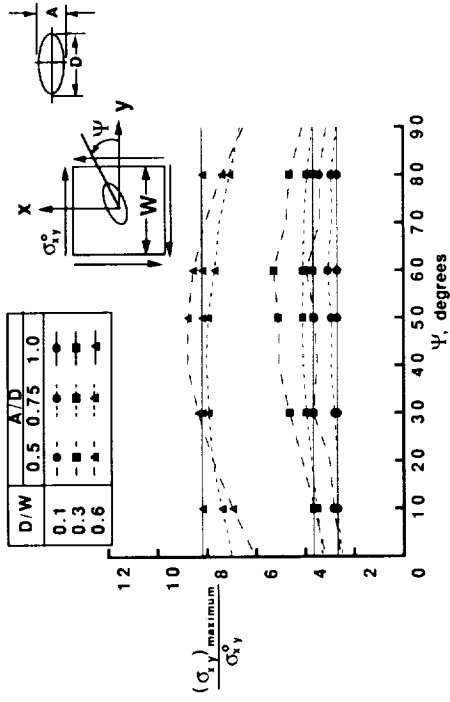


Fig. 21. Maximum shear stresses in a square shear-loaded [(±60)6]s laminate with an elliptical cutout inclined to the y-axis.

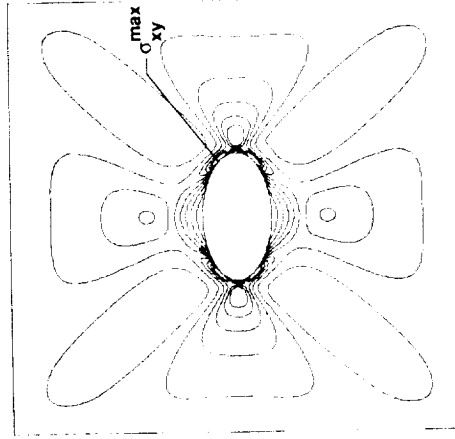


Fig. 22. Shear stress distribution for a square shear-loaded [(±45)6]s laminate with an elliptical cutout aligned with the y-axis.

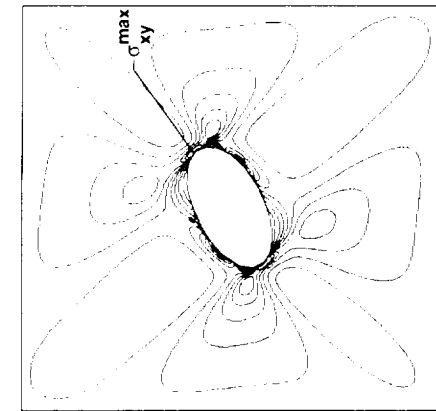


Fig. 23 Shear stress distribution for a square shear-loaded $[(\pm 45)_6]_s$ laminate with an elliptical cutout inclined at 25° to the y-axis.

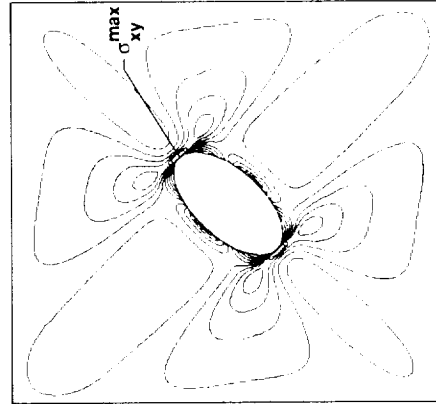


Fig. 24 Shear stress distribution for a square shear-loaded $[(\pm 45)_6]_s$ laminate with an elliptical cutout inclined at 45° to the y-axis.

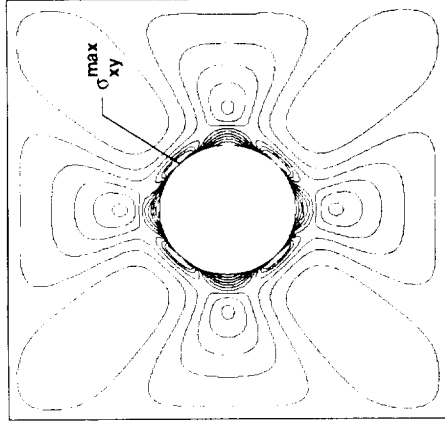


Fig. 25 Shear stress distribution for a square shear-loaded $[(\pm 45)_6]_s$ laminate with a circular cutout.

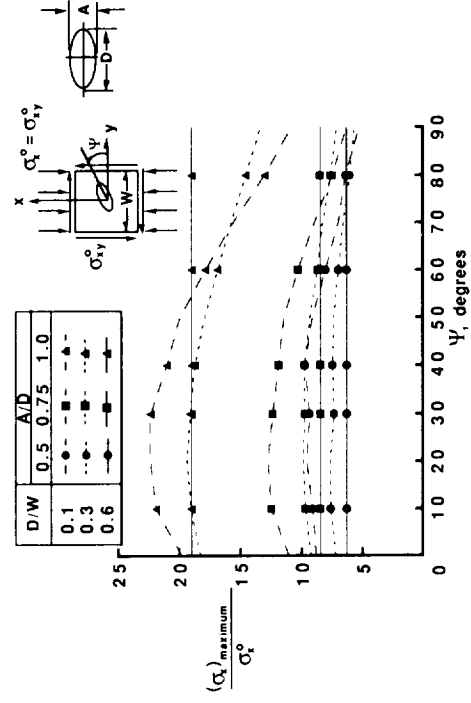


Fig. 26. Maximum normal stresses in a square compression- and shear-loaded $[(\pm 30)_6]_s$ laminate with an elliptical cutout inclined to the y-axis.

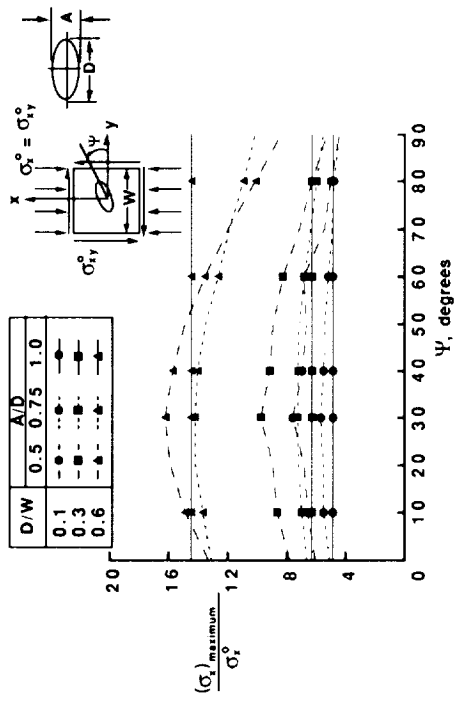


Fig. 27. Maximum normal stresses in a square compression- and shear-loaded [(±45)₆]_s laminate with an elliptical cutout inclined to the y-axis.

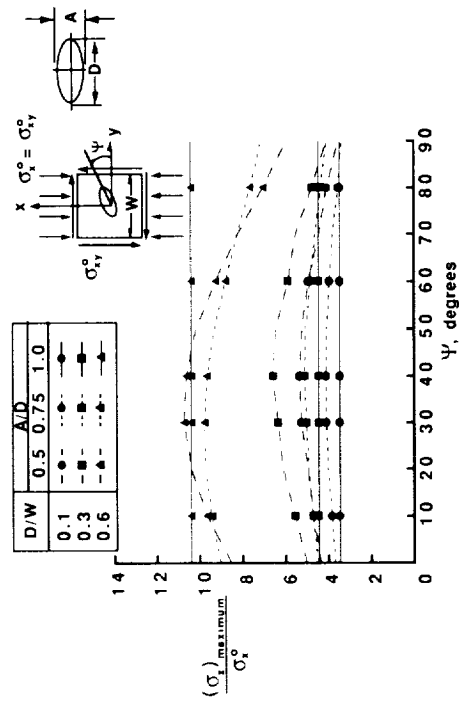


Fig. 28. Maximum normal stresses in a square compression- and shear-loaded [(±60)₆]_s laminate with an elliptical cutout inclined to the y-axis.

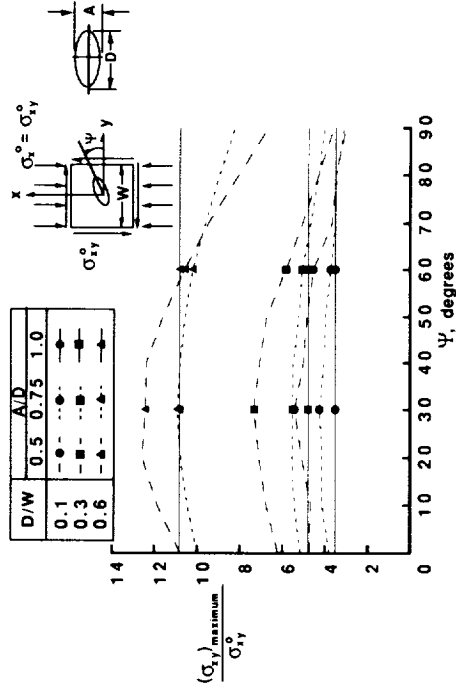


Fig. 29. Maximum shear stresses in a square compression- and shear-loaded [(±30)₆]_s laminate with an elliptical cutout inclined to the y-axis.

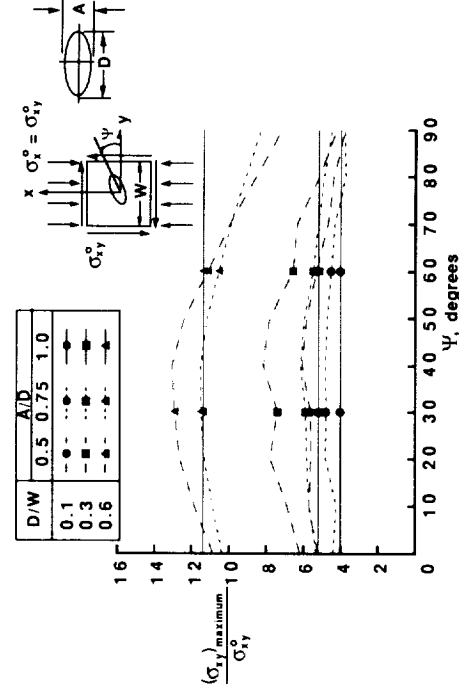


Fig. 30. Maximum shear stresses in a square compression- and shear-loaded [(±45)₆]_s laminate with an elliptical cutout inclined to the y-axis.

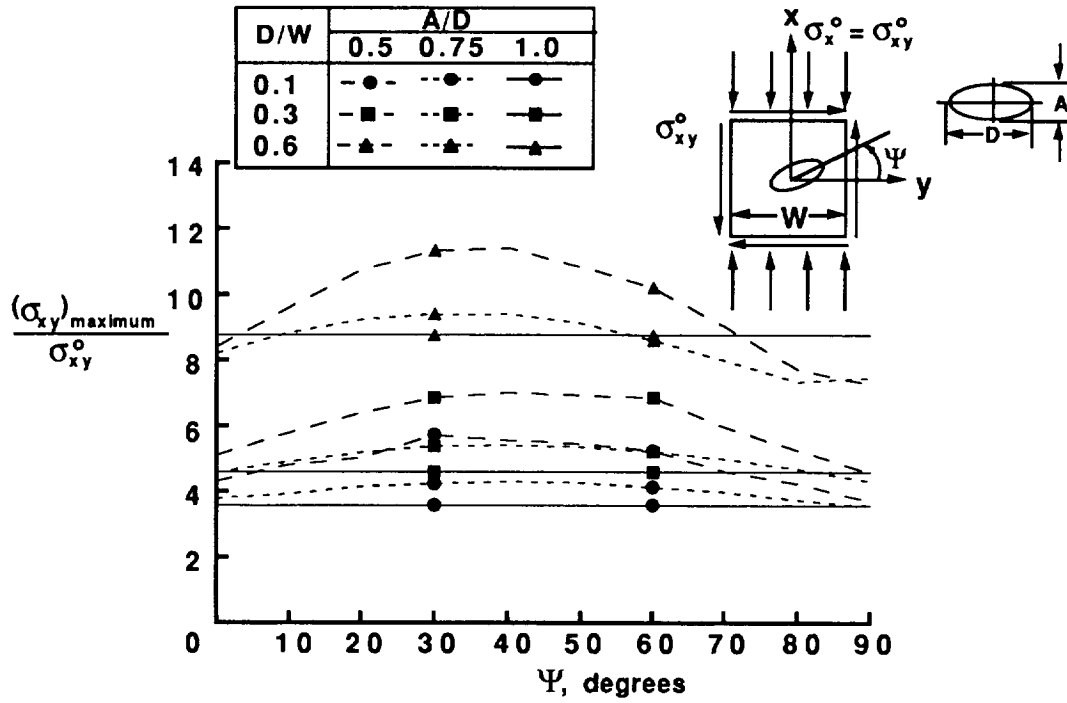


Fig. 31. Maximum shear stresses in a square compression- and shear-loaded $[(\pm 60)_6]_s$ laminate with an elliptical cutout inclined to the y-axis.

THIS PAGE INTENTIONALLY BLANK